Phase Separation of Binary Polymer Blends Driven by Photoisomerization: An Example for a Wavelength-Selection Process in Polymers

Takashi Ohta, Osamu Urakawa,† and Qui Tran-Cong*

Department of Polymer Science and Engineering, Kyoto Institute of Technology, Matsugasaki, Kyoto 606, Japan

Received March 12, 1998; Revised Manuscript Received August 6, 1998

ABSTRACT: Phase separation of polystyrene derivatives (PSS) and poly(vinyl methyl ether) (PVME) mixtures was induced in the one-phase region by using photoisomerization of *trans*-stilbene moieties labeled on the PSS chains. The phase separation was monitored by phase-contrast optical microscopy and was analyzed using digital image analysis under various experimental conditions such as temperature, light intensity, and the blend composition. During the reaction, the spontaneous pinning of the phase separation process was observed as predicted by the linear stability analysis of the time-dependent Ginzburg−Landau equations (TDGL) proposed recently for chemically reacting systems. The photoisomerization in the one-phase region of the blends does not follow the mean-field kinetics and can be well expressed by the Kohlrausch−Williams−Watts mechanism. By varying the annealing time and the reaction rates, it was found that the elastic stress resulting from the reaction inhomogeneity plays a key role in the emergence of lamella-like morphology. The correspondence between the phase separation of polymer blends accompanied by a reversible reaction and the microphase separation of diblock copolymers is discussed by comparing these experimental data with recent simulation using the TDGL equation for reacting mixtures. Finally, the morphology control based on phase separation induced by reversible reactions is discussed in terms of a wavelength selection process.

I. Introduction

Morphology control of multiphase polymers has been a long-standing research subject in polymer science due to its practical importance.[1] Since polymer blends are not miscible in most cases, their morphologies, in practice, are often controlled by introducing appropriate chemical reactions to the domain interfaces so that the domain sizes can be regulated by modifying the interfacial tension. In general, the morphologies of multiphase materials can be characterized by two principal factors: the characteristic length scale and the regularity of the structures. For the phase separation process developing from miscible blends, the former can be controlled by varying thermodynamic quantities such as quench depths or polymer diffusion, whereas the latter requires some sort of spatial symmetry breaking of the order parameter.[2] Therefore, the most efficient way of controlling morphology requires the regulation of both the wavelengths as well as the symmetry of these instabilities.

In the past few years, we have utilized photo-cross-linking reactions to control the time-evolution process of the spinodal decomposition in binary polymer blends.[3] It was demonstrated in these works that the unstable modes developing during the spinodal process can be suppressed by photo-cross-linking reactions between polymer chains of one polymer component. As a result, the phase separation can be frozen at an intermediate stage of the spinodal decomposition. In these particular cases, the length scales of the morphology could be controlled by experimentally adjusting the reaction rates and the growth rates of the phase separation process.[4] In other words, the fluctuations with long wavelengths, the so-called soft modes, via which the final morphology is determined, can be selected and controlled by the competitions between the cross-linking reaction and the phase separation. These experimental results reveal the possibility of using cross-linking reactions as a "modes tuner" for the wavelength selection process[5] in polymer mixtures.

Recent analytical theories and computer simulations show that a spontaneous pinning process can also take place in the phase separation of binary mixtures accompanied by a reversible reaction due to the mechanism of soft-mode suppression.[6] Furthermore, from the mathematical analogy between the equations of motion, it was also shown that there exists a similarity between the morphology resulting from macrophase separation of binary mixtures undergoing reversible reactions and the microphase separation of diblock copolymers.[7] More recently, the phase separation behavior of binary mixtures induced by reversible reactions was analyzed in a more general way by introducing chemical reaction terms into the Cahn−Hilliard equation under stationary nonequilibrium conditions.[8] The analytical solutions show that under some restricted conditions determined by the reaction kinetics and the thermodynamics of the mixture, the long wavelength fluctuations might be suppressed, leading to the formation of a stationary structure with an intrinsic length scale. However, the theoretical models proposed so far only consider the fundamental aspects of reaction−diffusion equations for small molecule systems where the unique features of polymer materials such as elasticity and nonhomogeneous kinetics of the reactions were not taken into account. Therefore, it is of great interest to examine if the unstable modes determining the final morphologies of polymer mixtures can be selected and controlled by reversible chemical reactions. Recently, in a prelimi-

* To whom correspondence should be addressed.
† Current address: Department of Macromolecular Science, Graduate School of Science, Osaka University, Osaka 560-0043, Japan.

S0024-9297(98)00394-5 CCC: $15.00
Published on Web 09/17/1998

nary experiment, it was found that the long wavelength fluctuations in polystyrene/poly(vinyl methyl ether) blends can be suppressed by the photoisomerization of stilbene labeled on polystyrene chains.[9]

In this paper, the phase separation of stilbene-labeled polystyrene/poly(vinyl methyl ether) (PSS/PVME) blends induced by irradiation with UV (ultraviolet) light was examined in great detail to elucidate the soft-mode suppression process predicted by the current theories. The morphology and the phase separation kinetics were investigated under a variety of experimental conditions such as light intensity, temperature, the blend composition, and the excitation wavelengths. The contribution of the elastic stress associated with the structural modification of the PSS chains due to the photoisomerization was examined by using irradiation-annealing cycles. These results were subsequently compared to the data obtained recently by computer simulation. The correlation between macrophase separation of polymer blends induced by reversible reactions and the microphase separation of block copolymers was also investigated by following the phase separation processes in polymer blends with various compositions induced by different light intensities. Finally, the role of elastic stress associated with the reaction inhomogeneity is discussed.

II. Experimental Section

1. Samples. Polymer blends used in this work are the mixtures of *trans*-stilbene-labeled polystyrene (PSS, $M_w = 3.2 \times 10^5$, $M_w/M_n = 1.7$) and poly(vinyl methyl ether) (PVME, SP[2], $M_w = 9.5 \times 10^4$, $M_w/M_n = 2.6$). PSS was prepared by the following procedure. At first, polystyrene was chloromethylated by copolymerizing styrene with a small amount of (chloromethyl)styrene (Tokyo Kasei) according to the method reported previously.[10] Potassium salt of *trans*-4-hydroxystilbene (4S-OH, Lancaster Synthesis Ltd., recrystallized twice in toluene) was prepared by reacting 4S-OH with potassium carbonate (Wako Chemicals) in methanol at room temperature over 3 h. Subsequently, the dried potassium salt of 4S-OH was reacted with the chloromethylated polystyrene in anhydrous dimethylformamide (Aldrich) at 65 °C over 6 h. The stilbene-labeled polystyrene was finally obtained by pouring the reacting solutions into iced water and then filtered. Prior to blending with PVME, PSS was precipitated twice using tetrahydrofuran as a good solvent and methanol as the nonsolvent. The label content of the PSS chains is determined by using the molar extinction coefficient of the model compound *trans*-4-methoxystilbene (Sigma, recrystallized twice in toluene) and was found as 1 stilbene per 20 repeat monomer units of the PSS chains. The chemical structures of the two polymers and the photoisomerization of stilbene are shown in Figure 1. The blends were prepared by casting toluene solutions containing appropriate amounts of PSS and PVME and were dried over 2 days in vacuo at 60 °C to remove residual solvents. Finally, the samples with the dimension (12 mm × 6 mm × 0.05 mm) were sandwiched between two quartz plates prior to the irradiation experiments.

2. Irradiation Experiments. PSS/PVME blends were irradiated with a 250 W Hg−Xe lamp (Model MUV-202U, Moritex, Japan) through an optical fiber system. The two lines 313 and 365 nm were selected and used to induce the photoisomerization of stilbene in PSS/PVME blends placed in a brass heating block

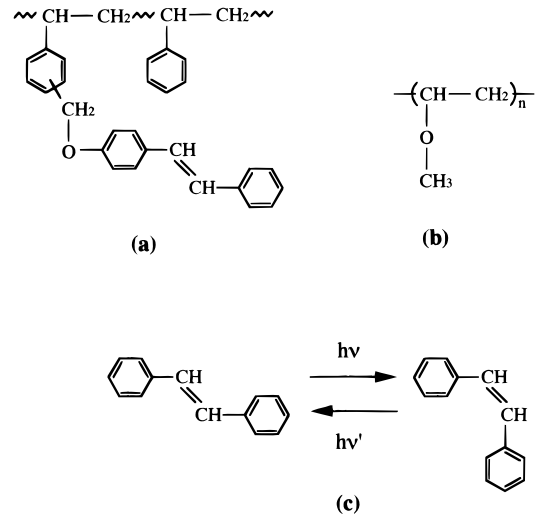

Figure 1. Chemical structures of stilbene-labeled polystyrene derivatives (a), poly(vinyl methyl ether) (b), and photoisomerization of stilbene (c).

with a quartz window. The temperature was thermostated with a precision of ±0.2 °C by using a temperature controller (Model EC-5600, Okura Electrics Co.). To ensure thermal equilibrium, all the samples were kept in the dark for 3 min at a given temperature prior to irradiation.

3. Morphological Observation and Data Analysis. The morphology emerging after irradiation over a certain period of time was observed by using a phase-contrast optical microscope (Nikon, Model FTX-21) . The optical images were digitalized and stored in a digital image analyzer (Pias LA-525). Subsequently, these data were transferred to a Macintosh computer (Power Mac 7100/80AV) and were analyzed by two-dimensional fast Fourier transform (2D-FFT) using standard softwares for image analysis (Scion Images and Super Paint). The corresponding one-dimensional (1D) power spectra of the images were obtained either by circular or sector average of the corresponding 2D data. The characteristic length scales ξ of the morphology were then calculated by using the Bragg formula $\xi = 2\pi/q_{max}$, where q_{max} is the frequency at the maximum power spectra. Finally, the data obtained from the Fourier transform are compared to the original images to justify the analysis.

4. Photoisomerization Kinetics of Stilbene in PSS/PVME Blends. Photoisomerization kinetics of *trans*-stilbene labeled on PSS chains in the blends was monitored at 355 nm by using a UV−visible spectrophotometer (UV-160, Shimadzu). Since the absorption spectra of *trans*-stilbene overlap with those of its *cis*-isomer, the changes in the concentrations of the *trans*-isomers with irradiation time were obtained by using the following procedure. Taking into account that all the stilbene moieties labeled on PSS chains are *trans*-isomers before irradiation, the initial absorbance OD_0 measured at a given wavelength can be written as

$$OD_o = \epsilon_t C_o d \tag{1}$$

where d is the sample thickness. ϵ_t and C_o are respectively the molar extinction coefficient and the molar concentration of the *trans*-isomer.

The absorption monitored at a given wavelength after an irradiation time t is the sum of the contribution of

both the *trans*- and *cis*-isomers in the blend:

$$\mathrm{OD}(t) = \mathrm{OD}_t(t) + \mathrm{OD}_c(t)$$
$$= \epsilon_t C_t d + \epsilon_c C_c d \quad (2)$$

Here C_t and C_c are respectively the molar concentrations of *trans*- and *cis*-stilbenes measured after t min of irradiation. ϵ_t and ϵ_c, the molar extinction coefficients of these two isomers, were estimated from the absorption data of the model compound 4-methoxystilbene in the literature.[11] By combining eqs 1 and 2 and the conservation law $C_o = C_t(t) + C_c(t)$, the molar concentrations of the two isomers after a given irradiation time t can be obtained. For convenience, the reaction kinetics was analyzed using the irradiation time dependence of the *trans*-isomer fraction measured at 355 nm.

5. Prediction from the Time-Dependent Ginzburg−Landau Equation for Binary Mixtures Undergoing Reversible Reactions. The time evolution of phase separation in binary mixtures accompanied by the reversible reaction

$$\mathrm{A} \underset{k_b}{\overset{k_f}{\rightleftharpoons}} \mathrm{B} \quad (3)$$

can be expressed by the following time-dependent Ginzburg−Landau equation:[6]

$$\frac{\partial\phi(r,t)}{\partial t} = M\nabla^2\frac{\delta f\{\phi(r,t)\}}{\delta\phi(r,t)} + g(\phi) \quad (4)$$

where $\phi(r,t)$ is the order parameter and M is the mutual mobility. $g(\phi)$ is the contribution of the reaction term given by $g(\phi) = -k_f\phi + k_b(1 - \phi)$ for the particular reaction shown in (3). $f\{\phi(r)\}$ is the Cahn−Hilliard type free energy of the mixture:[12]

$$f\{\phi(r)\} = \int \mathrm{d}r\, \{f_o[\phi(r)] + \kappa[\nabla\phi(r)]^2\} \quad (5)$$

Here f_o is the local, uniform free energy of the mixture and the second term in the right-hand side (rhs) of (5) is the square-gradient term with the interfacial free-energy coefficient κ.

Equation 4 predicts two important aspects of the phase separation for binary mixtures associated with the reversible reaction 3.

(a) Suppression of the Long Wavelength Fluctuations. For the case $k_f = k_b = k$, the following dispersion relation can be derived from the linear stability analysis of eq 4:[6]

$$R(q) = Mq^2\left[-\left(\frac{\partial^2 f}{\partial\phi^2}\right) - 2\kappa q^2\right] - 2k \quad (6)$$

Without the reaction term ($-2k$), eq 6 is the dispersion relation of the Cahn−Hilliard theory[12] for unreacted binary mixtures. The presence of the reaction term ($-2k$) makes the time evolution of the phase separation unique. Namely, the growth rate $R(q)$ of fluctuations becomes negative at the wavenumber $q = 0$, suggesting that the fluctuations with very long wavelengths, i.e., the soft modes, are suppressed by the chemical reaction. Physically, the theory suggests that the spontaneous pinning of phase separation will occur and a stationary modulated structure characterized by an intrinsic wavenumber q_e emerges as a consequence of the competition between the reaction and phase separation. Recently, a modified Cahn−Hilliard equation containing a reversible reaction operated under nonequilibrium conditions by contact with external reservoirs was developed and analytically solved within the linear region of phase separation.[8] It was found that under these general conditions, the soft-mode suppression does not always exist and only occurs under a limited condition determined by thermodynamics and the reaction kinetics.

(b) Correlation between the Macrophase Separation of Polymer Mixtures Accompanied by a Reversible Reaction and the Microphase Separation of Block Copolymers. It was shown that for the TDGL eq 4 with $k_f = k_b = k$, the reaction term $g(\phi)$ can be incorporated into the free-energy functional $f\{\phi(r)\}$ and rewritten as[7,13,14]

$$\frac{\partial\phi(r,t)}{\partial t} = M\nabla^2\frac{\delta F\{\phi(r,t)\}}{\delta\phi} \quad (7)$$

where

$$F\{\phi(r,t)\} = f\{\phi(r,t)\} + \frac{k}{M}\int\int G(r,r')\,\phi(r,t)\,\phi(r',t)\,\mathrm{d}r\,\mathrm{d}r' \quad (8)$$

The free energy $F\{\phi(r,t)\}$ is composed of two terms: the first term comes from the phase separation (eq 5) and the second term with the Green function $G(r,r')$ expressing the comparatively long-range effects of the chemical reaction. Equation 7 with the free energy containing the nonlocal term given by (8) has been successfully used to explain the emergence of the so-called modulated phases in a wide variety of systems where there exists the competing interactions including block copolymers.[15] For reacting polymer blends, these equations are accidentally identical to the equation of motion with the free energy proposed for the microphase separation of diblock copolymers[16,17] where

$$\left(\frac{k}{M}\right) \propto \frac{1}{[Nf(1-f)]^2} \quad (9)$$

Here, N and f are the degree of polymerization and the block ratio, respectively. Equation 9 suggests that by changing the ratio (k/M), morphologies such as hexagonal and lamellar, which are often observed for microphase separation of diblock copolymers, can emerge in chemically reacting polymer blends at the micrometer scale. Here, this theoretical prediction is experimentally examined by varying the initial composition of the reacting blend and by changing the reaction rate at a fixed temperature.

III. Results and Discussion

1. Phase Behavior of PSS/PVME Blends. The cloud points of *trans*-stilbene-labeled polystyrene and poly(vinyl methyl ether) (PSS/PVME) blends were measured by light scattering at a fixed angle (20°). To minimize the kinetic effects associated with the slow diffusion of polymers, these cloud points were observed at 0.5, 0.2, and 0.1 °C/min and then extrapolated to zero-heating rate to obtain the final data. The results are shown in Figure 2 together with the glass transition temperatures (T_g) measured by differential scanning calorimetry (dsc) with a heating rate of 5 °C/min. From these results, it was found that PSS/PVME blends undergo phase separation upon increasing temperature

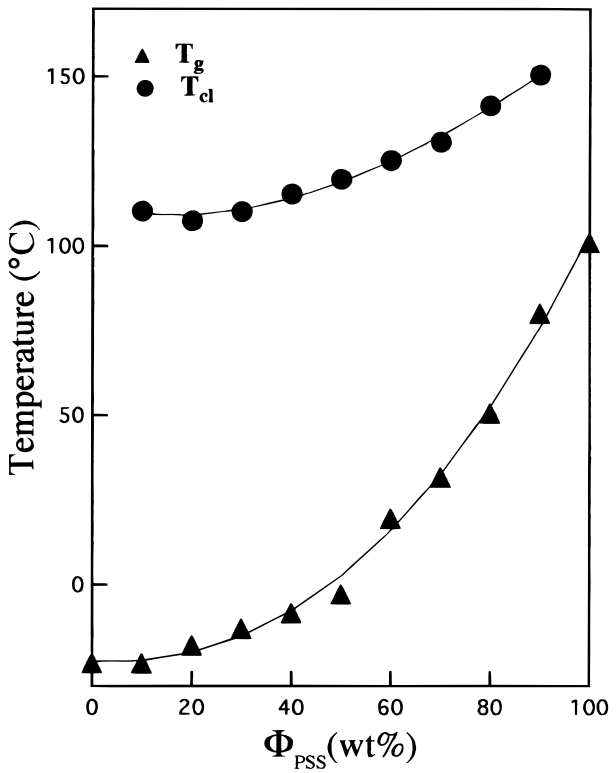

Figure 2. Cloud points (T_{cl}) and glass transition temperatures (T_g) of PSS/PVME blends measured by light scattering and differential scanning calorimetry, respectively.

with the critical point in the vicinity of $\phi_{PSS} = 0.2$. All the experiments were carried out within the one-phase region limited by the cloud point curve and the glass transition temperatures.

2. Effects of the Light Intensity on the Phase Separation Kinetics. It is well-known that stilbene undergoes reversible photoisomerization upon irradiation with UV light.[18] Since the changes in molecular volume as well as dipole moment are associated with the conformational transitions from the planar form (the *trans*-isomer) to the bulky state (the *cis*-isomer), an attempt to utilize the photoisomerization of stilbene to control the phase separation of polymer blends was reported previously.[19] The thermodynamical destabilization of PS/PVME blends induced by the photoisomerization of stilbene has been attributed to the increase in molecular volume associated with the *trans* → *cis* photoisomerization. More recently, it was found from the χ parameter obtained by small-angle neutron scattering that the difference in enthalpic interactions between the *trans*-isomer/PVME and the *cis*-isomer/PVME segments is also responsible for this thermodynamic instability.[20]

Upon irradiation with UV light (313 nm, 0.1 mW/cm^2), a PSS/PVME (20/80) blend undergoes phase separation. The morphology becomes observable under a phase-contrast optical microscope after 400 min of irradiation. As an example, the morphologies and their corresponding power spectra obtained by 2D-FFT under irradiation over various periods of time are shown in Figure 3. As irradiation time increases, the structures become coarsened and eventually are almost unchanged with time after 1500 min of irradiation. The morphologies induced by the photoisomerization under this experimental condition are almost isotropic, as revealed by the 2D-FFT power spectra. On the other hand, a PSS/PVME (20/80) blend irradiated with a higher intensity, 4.1 mW/cm^2, exhibits anisotropic morphology after 200 min of irradiation. The structural anisotropy without preferential directions becomes more obvious with increasing irradiation time. Shown in Figure 4 are the morphologies of a PSS/PVME (20/80) blend obtained after 360 min of irradiation at 90 °C using 313 nm UV light with the intensity varying from 0.5 to 4.1 mW/cm^2. The corresponding 2D-FFT power spectra show a tendency that for the same composition and temperature, the resulting morphology turns from isotropic to lamella-like structures as the irradiation intensity increases.

To follow the effects of the light intensity on the phase separation kinetics, the characteristic length scale ξ of the morphologies obtained under various irradiation conditions was calculated from the 2D-FFT data according to the procedure described in section II.3. As illustrated in Figure 5, the temporal evolution of the PSS/PVME (20/80) blends shares a common feature. At the early stage, ξ is almost unchanged while the contrast increases with irradiation time. From the linear stability analysis described in section II.5, the early stage kinetics of phase separation associated with a reversible reaction can be expressed by an exponential function of reaction time $\phi(q,t) \propto \exp[R(q)t]$, where $R(q)$ might be given by eq 6. Therefore, the region where the length scale ξ of the morphology is almost unchanged before increasing with reaction time shown in Figure 5, probably reflects the linear region resembling the Cahn−Hilliard linearized theory for nonreacting systems.[12] At a later time, the structures gradually grow with irradiation time according to the Lifshitz−Slyosov−Wagner (LSW) power law[21,22] $\xi \propto t^{\alpha}$ with α approximately equal to 1/3. Eventually, ξ approaches an equilibrium length scale ξ_{eq} that changes with the light intensity. For the anisotropic morphology obtained with the highest intensity 4.1 mW/cm^2, ξ was calculated from the 1D data of the power spectra extracted along the direction perpendicular to the lamellar structures. The existence of the equilibrium length scales at long irradiation time reveals the spontaneous pinning process of the phase separation of PSS/PVME (20/80) blends induced by photoisomerization of stilbene. There are two possibilities for this particular behavior of the phase separation. One is coming from the decrease of mobilities in the PSS-rich domains forming in the late stage of irradiation. The other may be caused by the soft-mode suppression arising from the *trans* ⇄ cis photoisomerization of stilbene, as theoretically predicted.[6,8] By modifying the ratio of the forward to the backward reaction rates via changing the excitation wavelength, the evidence for this spontaneous pinning process becomes more obvious, as described below.

From the viewpoint of phase separation kinetics, a PSS/PVME (20/80) blend moves faster into the unstable region upon irradiation with high intensity. The phase separation under this particular condition corresponds to a "deep quench" process, whereas it satisfies the "shallow quench" by irradiation with low intensities. However, this interpretation is not completely supported by the experimental results depicted in Figure 5 because the equilibrium length scales increase with increasing light intensity, in contrast to the phase separation kinetics observed under deep quench conditions. This time evolution suggests that there may exist another physical process simultaneously effecting the phase separation kinetics besides the chemical reaction.

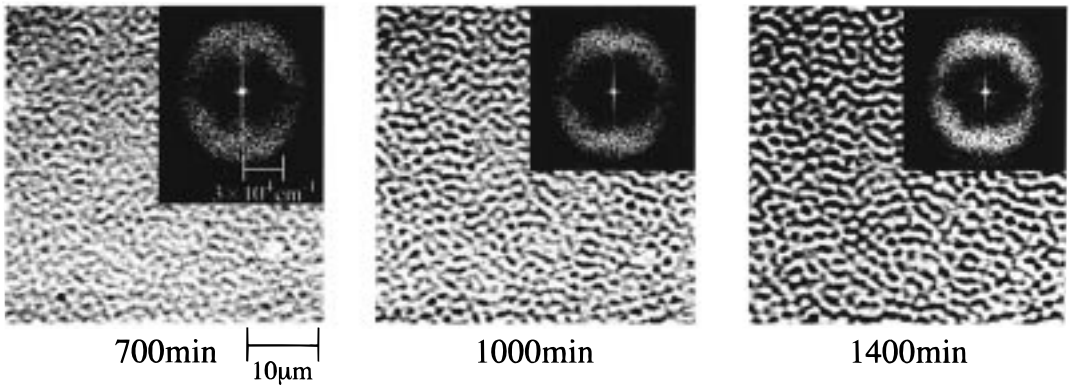

Figure 3. Time evolution of the phase separation observed for a PSS/PVME (20/80) blend irradiated at 90 °C with 313 nm UV light. The light intensity is 0.1 mW/cm^2.

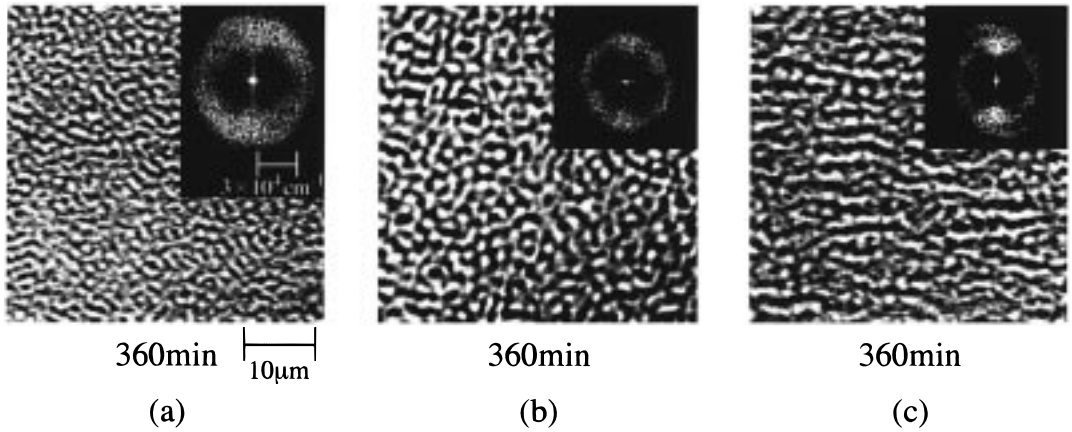

Figure 4. Effects of the light intensity on the morphology of PSS/PVME (20/80) blends irradiated at 90 °C with 313 nm UV light: (a) 0.5 mW/cm^2; (b) 1.6 mW/cm^2; (c) 4.1 mW/cm^2. The numbers below the figures indicate irradiation time.

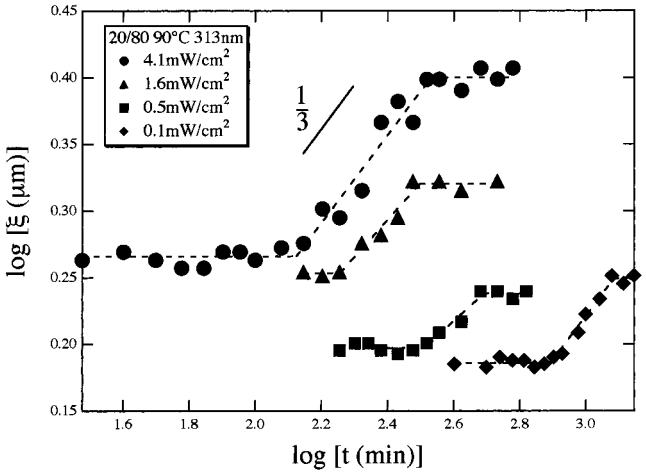

Figure 5. Dependence of the phase separation kinetics on the light intensity observed for a PSS/PVME (20/80) blend irradiated at 90 °C with 313 nm UV light.

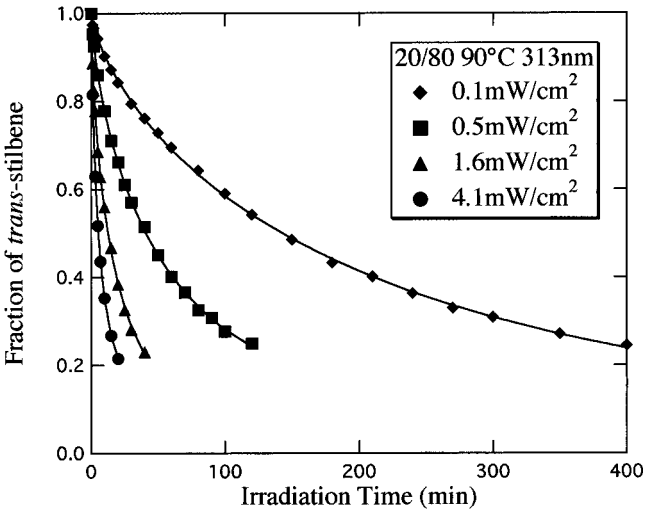

Figure 6. Dependence of the photoisomerization kinetics on the light intensity observed for a PSS/PVME (20/80) blend irradiated at 90 °C with 313 nm UV light. The solid curves were obtained by fitting the data to the modified KWW equation (10).

3. Photoisomerization Kinetics of Stilbene in the Miscible Region of PSS/PVME Blends. To confirm the above hypothesis, the photoisomerization kinetics of stilbene was monitored during irradiation until the blends start undergoing phase separation. Figure 6 shows the irradiation time dependence of the *trans*-stilbene fraction in PSS/PVME (20/80) blends irradiated at 90 °C with the experimental conditions shown in Figure 6. These fractions were estimated according to the procedure described in section II.4. It was found that the *trans* ⇄ *cis* photoisomerization of stilbene in these PSS/PVME (20/80) blends does not follow the first-order kinetics, implying that the reaction does not proceed homogeneously in the sample under irradiation. These results are consistent with the nonhomogeneous kinetics of photoisomerization observed previously with azobenzene in the bulk state of homopolymers.[23,24] To estimate the reaction rates of stilbene in these blends, the irradiation time dependence

Table 1. Kinetic Parameters Obtained by Fitting the Fraction $C(t)$ of *trans*-Stilbene to the Stretched Exponential Function (10) for a PSS/PVME (20/80) Blend Irradiated with UV Light at 90 °C[a]

	light intensity (mW/cm^2)			
	0.1	0.5	1.6	4.1
k_o (min^{-1})	0.0045	0.018	0.052	0.167
β	0.73	0.74	0.70	0.82
B	0.032	0.087	0.042	0.224

[a] The excitation wavelength is 313 nm.

of the *trans*-isomer fraction was fitted to the modified stretched exponential (Kohlrausch−Williams−Watts) function:[25]

$$C(t) = \frac{C_t(t)}{C_o} = [1 - B]e^{-(k_o t)^\beta} + B \qquad (10)$$

where C_o and $C_t(t)$ are the molar concentrations of *trans*-stilbene isomer before and after t min of irradiation. $C(t)$ is the normalized concentration of the *trans*-isomer. k_o, β, and B are respectively the average reaction rate, the inhomogeneity index of the reaction, and the baseline expressing the equilibrium of the reaction under a given excitation wavelength.

It was found that all the irradiation time dependence of *trans*-stilbene in PSS/PVME (20/80) blends can be well expressed by eq 10. The kinetic parameters obtained from the curve fitting are summarized in Table 1. The significant variation of the profiles of $C(t)$ with the light intensity observed within a fixed time scale might distort the systematic dependence of the fitting parameters β and B on irradiation time.

Nevertheless, the rate of the photoisomerization increases almost 40 times as the intensity changes from 0.1 to 4.1 mW/cm^2. Because the photoisomerization of stilbene induces changes in the chemical structures of the PSS chains, the reaction inhomogeneity might lead to the formation of some local gradients of elastic stress in the reacting blend. Upon irradiation with intense UV light, the reaction proceeds quickly so that these gradients are amplified, resulting in anisotropic morphology, as shown in Figure 4c. As described later, the effects of elastic stress on the morphology induced by the fast photoisomerization become obvious when irradiation is combined with annealing experiments.

4. Effects of Temperatures on the Phase Separation Kinetics. Phase separation of PSS/PVME (20/80) blends induced by irradiation at low temperatures corresponds to a shallow quench process because the phase boundary of the mixtures only slowly approaches the experimental temperatures. The irradiation−time dependence of the characteristic lengths ξ of PSS/PVME (20/80) blends obtained by irradiation at 90 and 100 °C is shown in Figure 7. The phase separation kinetics exhibits similar behavior for both temperatures. ξ is almost unchanged at the early stage of the phase separation, then increases with irradiation time according to the LSW growth law with $\alpha = 1/3$, and eventually approaches an equilibrium length scale. At a higher temperature, the phase separation starts at earlier time and reaches a smaller equilibrium length scale ξ_{eq}. The average reaction rate k_o obtained by fitting the experimental data to eq 10 increases ca. 35% as temperature varies from 90 to 100 °C. Under irradiation with the highest intensity 4.1 mW/cm^2, the anisotropy of the morphology induced by photoisomerization of stilbene

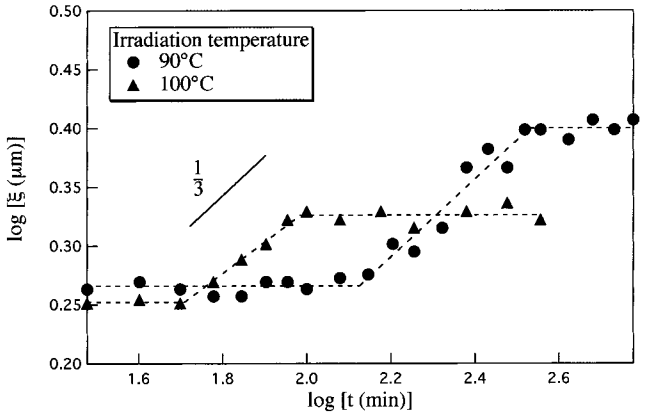

Figure 7. Temperature dependence of the phase separation kinetics of a PSS/PVME (20/80) blend irradiated with 313 nm UV light. The light intensity is 4.1 mW/cm^2.

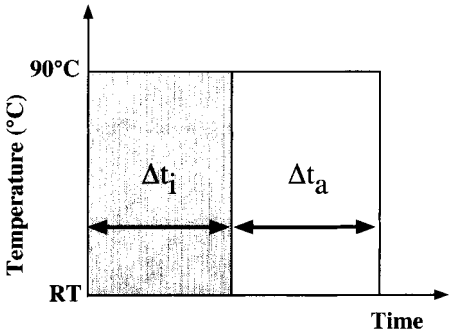

Figure 8. Schematic presentation of an irradiation−annealing cycle. Δt_i and Δt_a are respectively the duration of irradiation and annealing. RT: room temperature.

becomes insignificant above 100 °C. Relaxation of the elastic stress generated by the reaction inhomogeneity at temperatures above the T_g of the PSS component (101.0 °C) might be responsible for the disappearance of the morphological anisotropy. At lower temperatures, e.g., 70 °C, the phase separation proceeds very slowly, giving weakly anisotropic structures. The contrast of the morphology obtained at low temperatures is not strong because the phase separation takes place very slowly under these conditions. These results support the fact that phase separation induced at low temperatures corresponds to the shallow quench conditions and also imply that the anisotropy of the morphology originates from the local gradients of elastic stress that cannot completely relax at temperatures below the T_g of the PSS component.

5. Effects of Elastic Stress on the Resulting Morphology. As shown in Figure 4, the anisotropic morphology becomes remarkable when a PSS/PVME (20/80) blend is irradiated with the highest intensity 4.1 mW/cm^2, whereas it is not significant when lower intensities were used. To confirm the effects of the elastic stress induced by the reaction inhomogeneity on the blend morphology, experiments combining irradiation and annealing were carried out. A PSS/PVME (20/80) blend was first irradiated by 313 nm UV light with the intensity 4.1 mW/cm^2 over a period of time (Δt_i) and was subsequently annealed over a duration (Δt_a) at the same temperature with the light off, as schematically illustrated in Figure 8. This process was repeated and the morphology was monitored under a phase-contrast optical microscope after each irradiation−annealing cycle. Two durations of annealing $\Delta t_a = 10$ and 30 min

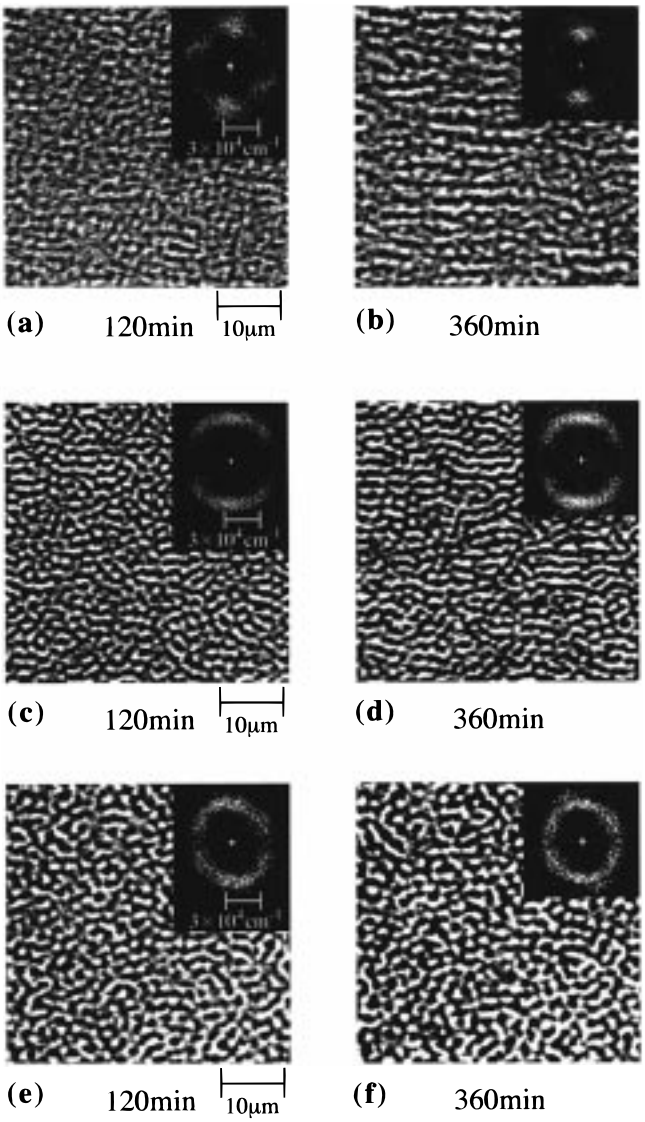

Figure 9. Effects of annealing time on the morphology of PSS/PVME (20/80) blends irradiated with UV light (313 nm, 4.1 mW/cm^2) at 90 °C: without annealing (a, b); annealing with $\Delta t_a = 10$ min (c, d) and 30 min (e, f). The numbers under the photographs indicate the total irradiation time. The total annealing times are respectively 300 and 780 min for the cases $\Delta t_a = 10$ min (c, d) and 300 min (e, f).

were chosen for each cycle. The morphological results were then analyzed and compared with a blend irradiated under the same conditions without annealing. Shown in Figure 9 are the morphologies and the corresponding 2D-FFT power spectra of PSS/PVME (20/80) blends experiencing the irradiation−annealing cycles at 90 °C with two durations $\Delta t_a = 10$ and 30 min. Compared to that of the blend irradiated under the same conditions without annealing (Figure 9a,b), the anisotropy of the morphology becomes less significant, as shown in Figure 9c,d, when the duration $\Delta t_a = 10$ min is applied to the blend after each time of irradiation. Furthermore, as illustrated in Figure 9e,f, the morphology of an irradiated PSS/PVME (20/80) blend is almost isotropic for $\Delta t_a = 30$ min. These data clearly suggest that the anisotropic morphology resulting from the photoisomerization induced with the light intensity 4.1 mW/cm^2 originates from the elastic stress associated with the inhomogeneity of the reaction. For the shorter annealing time ($\Delta t_a = 10$ min), the morphology is still

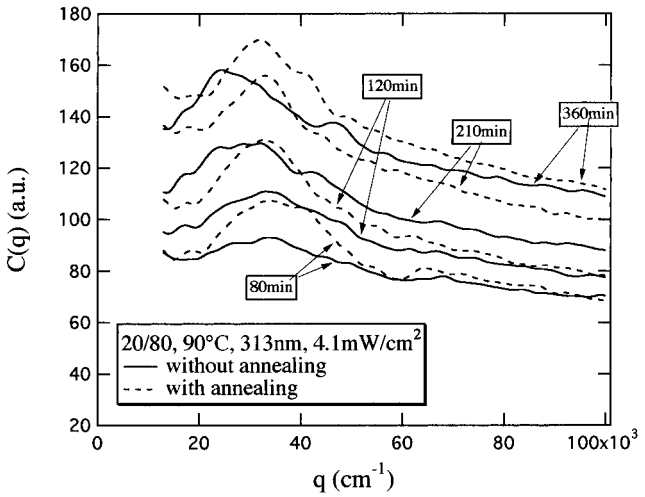

Figure 10. One-dimensional power spectra of a PSS/PVME (20/80) blend irradiated with UV light (313 nm, 4.1 mW/cm^2) at 90 °C: (—) without annealing; (- - -) with annealing.

partially anisotropic because the elastic stress cannot completely relax after each irradiation−annealing cycle. These experimental results reveal the important role of the elastic stress accompanying the structural changes of PSS chains in the blends during irradiation.

The time evolution of the 1D power spectra extracted from the 2D-FFT data is shown in Figure 10 for the cases of $\Delta t_a = 30$ and 0 min (without annealing) observed for PSS/PVME (20/80) blends irradiated with 4.1 mW/cm^2 UV light at 90 °C. Without annealing, the characteristic length ξ of the morphology grows with irradiation time in the fashion shown in Figure 5. However, by combining irradiation with annealing, the growth of these structures is significantly slowed, as observed in Figure 10. This slowing down of the phase separation in the presence of annealing is partially due to the *cis* → *trans* reverse process because the absorbance of stilbene monitored at 355 nm shows a small increase (less than 5%) after the whole annealing process. From the nonhomogeneous kinetics of the photoisomerization shown in Figure 6 and the *anisotropics* → *isotropic* morphological transition observed upon annealing in Figure 9, it can be concluded that the lamellar structures of PSS/PVME (20/80) blends obtained by irradiation with high intensity originate from the local gradients of elastic stress associated with the reaction inhomogeneity.

6. Soft-Mode Suppression Phenomena in Phase Separation of Polymer Blends Driven by Reversible Reactions. Since the photoisomerization is reversible upon irradiation with UV light and the rates of the forward and backward reactions can be controlled by selecting the excitation wavelength, it would be interesting to test the prediction of the soft-mode suppression described in section II.5. For this purpose, 365 nm UV light was used to induce the phase separation of PSS/PVME blends because the ratio of the two isomers is not significantly different at this particular wavelength. Upon irradiation with UV light at 365 nm (4.1 mW/cm^2), the phase separation of a PSS/PVME (50/50) blend becomes observable at 20 min after irradiation at 105 °C. It was found that the characteristic length scale ξ of these modulated structures is almost unchanged during the first 150 min of irradiation, as illustrated in Figure 11. As soon as the exciting light is turned off, these structures quickly grow, following

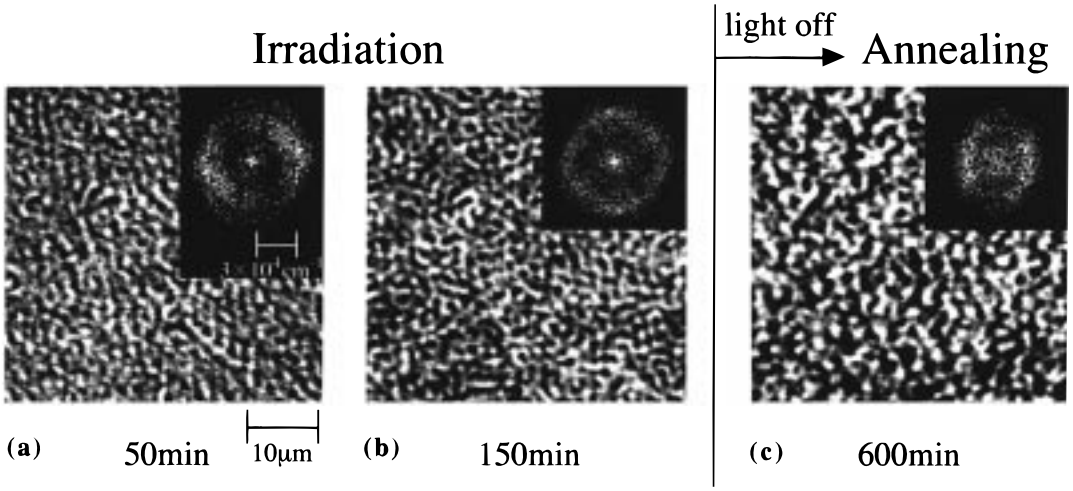

Figure 11. Morphological evidence for the soft-mode suppression in a PSS/PVME (50/50) blend irradiated with UV light (365 nm, 4.1 mW/cm^2) at 105 °C. Total irradiation time: (a) 50 min; (b) 150 min; (c) irradiation 150 min and annealing 450 min.

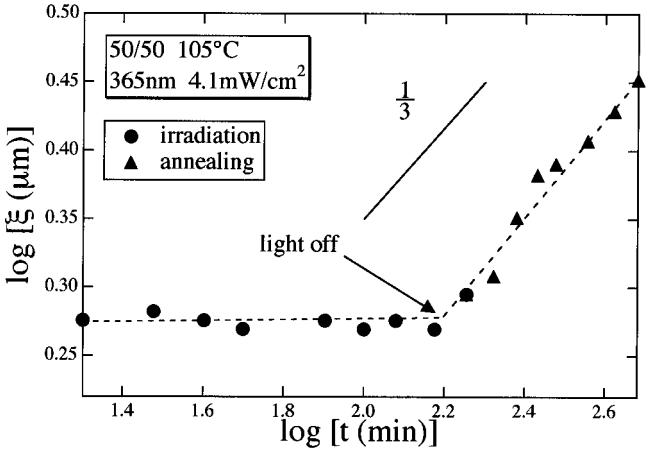

Figure 12. Time evolution of the characteristic length scale ξ of the PSS/PVME (50/50) blend shown in Figure 11 during irradiation (●) and under annealing in the dark (▲).

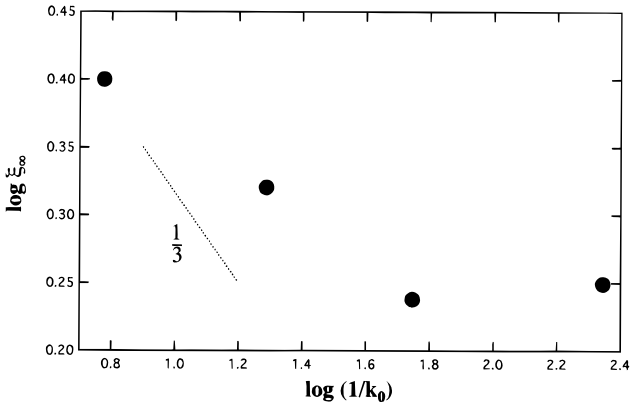

Figure 13. Dependence of the equilibrium length scale on the reaction rate k_o obtained from the results shown in Figures 5 and 6.

the Lifshitz−Slyosov−Wagner law with the exponent approximately equal to 1/3, as illustrated in Figure 12. These results indicate that the phase separation proceeds very slowly upon irradiation with 365 nm. Furthermore, since the experiments were carried out above the T_g of PSS, the pinning process due to the glassification of the PSS-rich domains during the phase separation can be ruled out. Therefore, we conclude that the fluctuations with long wavelengths, i.e., the soft modes, were suppressed by the photoisomerization of stilbene. The phase separation kinetic data shown in Figure 12 are in good agreement with the prediction from the linear stability analysis of the TDGL containing reversible reaction terms.[7,8,27]

Recently, the effects of the reaction rates on the phase separation associated with a reversible reaction were numerically studied by using the TDGL eq 4.[26] It was found that as the reaction rates increase, the suppression takes place at an earlier time. Contrary to the numerical calculation, the experimental data illustrated in Figure 5 and Table 1 show that the equilibrium length scales ξ_∞ achieved by the photoisomerization increase with increasing reaction rate. Analytically, it was shown that the intrinsic length scale ξ_∞ of the morphology can be scaled with the reaction rate k_o as $\xi_\infty \sim (1/k_o)^\alpha$, where α, the exponent of the LSW growth law, is equal to 1/3.[6] Experimentally, ξ_∞ obtained with the light intensity in the range 0.1−4.1 mW/cm^2 does not vary linearly with $(1/k_o)$ in double logarithmic scale as shown in Figure 13. Here, k_o is taken as the average reaction rate obtained by fitting the data of Figure 6 to the stretched exponential function (eq 10). Therefore, we conclude that the experimental data obtained in this work do not follow the theoretical prediction given by the TDGL equation (4). This disagreement probably originates from the contribution of elastic stress associated with the inhomogeneity of the reaction. The couplings between elastic stress and the concentrations in reacting polymer mixtures[28] remain as a key point for theoretical studies of phase separation induced by chemical reactions in polymer blends.

Since the *trans*-stilbene labeled PSS homopolymer was not phase- separated from its *cis*-counterpart upon irradiation with UV light above its T_g, it is reasonable to conclude that the phase separation observed with PSS/PVME blends is caused by the immiscibility between the *cis*-PSS and PVME. The UV light plays a role of switching the mixture between the two states: miscible and immiscible. As mentioned in section II.5, the TDGL equation (4) for the phase separation associated with a reversible reaction predicts that by changing the ratio (k/M) of the reaction rate to the mobility M, the morphology with the symmetry such as hexagonal or lamellar observed with block copolymers can be

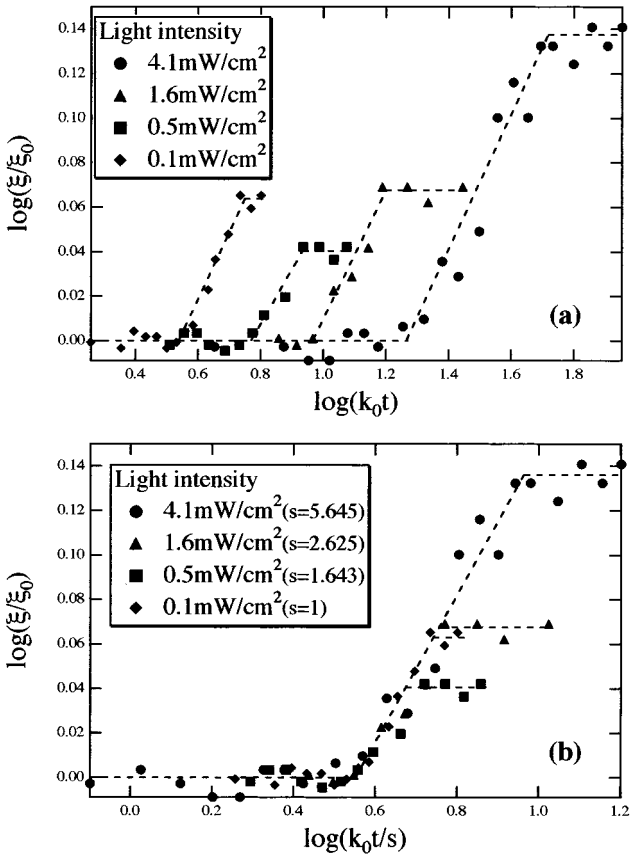

Figure 14. Reduced plots for the phase separation kinetics of PSS/PVME (20/80) blends under irradiation with the conditions indicated in Figure 5: (a) normalization using ξ_o and k_o; (b) normalization with the additional parameter s described in the text.

obtained, in principle, with reacting polymer blends. A PSS/PVME blend with an off-critical composition PSS/PVME (5/95) undergoes phase separation after 80 min of irradiation with UV light (313 nm, 4.1 mW/cm^2), exhibiting random phase-separated structures, and almost reaches phase equilibrium after 420 min, as revealed by 2D-FFT power spectra. Together with the dependence of the equilibrium length scale ξ_∞ on the average reaction rate k_o shown in Figure 13 and the large change in the reaction rate k_o with the light intensity, the above results seem to suggest that the phase separation of PSS/PVME blends driven by photoisomerization of stilbene does not follow the theoretical prediction provided by eqs 7 and 8.

7. On the General Behavior of the Phase Separation of PSS/PVME Mixtures Induced by Photoisomerization. As shown in Figure 5, the time evolution of the characteristic length scale ξ exhibits similar behavior under irradiation with the light intensities ranging from 0.1 to 4.1 mW/cm^2, suggesting that there might exist a certain general relationship for the phase separation driven by photoisomerization. As shown in Figure 14a, the normalized characteristic length scale (ξ/ξ_o) is plotted versus the reduced irradiation time ($k_o t$). Here, ξ_o is the intrinsic length scale that is unchanged with irradiation time observed in the early stage of phase separation, and k_o is the mean reaction rate taken from the analysis using Kohlrausch−Williams−Watts (KKW) kinetics in Figure 6. It was found that all the data obtained with these irradiation intensities do not superimpose on each other. However, when (ξ/ξ_o) was plotted versus ($k_o t/s$), where s is an adjustable parameter chosen so that $s = 1$ for the lowest intensity 0.1 mW/cm^2, all the data fall on a master curve, as illustrated in Figure 14b, except the equilibrium length scale ξ_∞. The adjustable parameter s increases with increasing irradiation intensity. These results clearly indicate that the phase separation kinetics of PSS/PVME (20/80) blends is not solely controlled by the light intensity, i.e., the rates of photoisomerization of stilbene. The annealing data shown in Figure 9 strongly suggest that the additional control parameter for this phase separation might be related to the elastic stress accompanying the structural changes induced by the reaction.

IV. Summary and Conclusion

Phase separation of poly(vinyl methyl ether) (PVME) and polystyrene derivatives (PSS) mixtures driven by photoisomerization of stilbene labeled on PSS chains was examined by phase-contrast optical microscopy combined with digital image analysis. The findings are as follows:

(1) PSS/PVME blends undergo phase separation induced by the *trans* ⇄ *cis* photoisomerization of stilbene, exhibiting spontaneous pinning during the reaction. The soft-mode suppression driven by this reversible reaction was experimentally observed, as predicted by the linear stability analysis of the Cahn−Hilliard equations modified for reacting mixtures.

(2) The photoisomerization of stilbene proceeds inhomogeneously in the reacting blends and can be well expressed by the Kohlrausch−Williams−Watts kinetics. By combining irradiation with annealing experiments, it was found that the resulting elastic stress associated with this reaction inhomogeneity is responsible for the emergence of the anisotropic morphologies upon irradiation with high intensity.

(3) The phase separation kinetics exhibits a common feature. The structures are almost unchanged with irradiation in the early stage and subsequently grow according to the Lifshitz−Slyozov−Wagner 1/3 power law. Eventually, the phase separation was frozen at long irradiation time.

(4) The mathematical equivalence between the macrophase separation of binary polymers driven by reversible chemical reactions and the microphase separation of diblock copolymers was not observed in the phase separation of PSS/PVME blends.

The above experimental results suggest that some theoretical models taking into account the couplings between the elasticity and the composition are currently in need of quantitatively interpreting the phase separation phenomena in polymer blends accompanied by reversible reactions.

Acknowledgment. The financial support from the Ministry of Education, Science, and Culture, Japan (Grant-in-Aid No. 09650998), is gratefully acknowledged.

References and Notes

(1) For example, see: (a) *Rubber-Toughened Plastics*; Riew, C. K., Ed.; Advances in Chemistry Series No. 222; American Chemical Society: Washington, DC, 1989. (b) *Toughened Plastics II: Novel Approaches in Science and Engineering*; Riew, C. K.; Kinloch, A. J., Eds.; Advances in Chemistry Series No. 252; American Chemical Society: Washington, DC, 1996.

(2) Tran-Cong, Q.; Kataoka, K.; Urakawa, O. *Phys. Rev. E* **1998**, *57*, R1243.
(3) Imagawa, A.; Tran-Cong, Q. *Macromololecules* **1995**, *28*, 8388.
(4) Harada, A.; Tran-Cong, Q. *Macromololecules* **1996**, *29*, 4801.
(5) Cross, M. C.; Hohenberg, P. C. *Rev. Mod. Phys.* **1993**, *65*, 861.
(6) Glotzer, S. C.; Di Marzio, A. E.; Muthukumar, M. *Phys. Rev. Lett.* **1995**, *74*, 2034. For review, see: (a) Glotzer, S. C. In *Annual Reviews of Computational Physics*; Stauffer, D., Ed.; World Scientific: Singapore, 1995; Vol. II, pp 1−46. (b) Bansil, R.; Liao; G. *Trends Polym. Sci.* **1997**, *5*, 146.
(7) Glotzer, S. C.; Cogniglio, A. *Phys. Rev. E* **1994**, *50*, 4241.
(8) (a) Lefever, R.; Carati, D.; Hassani, N. *Phys. Rev. Lett.* **1995**, *75*, 1674. (b) Carati, D.; Lefever, R. *Phys. Rev. E* **1997**, *56*, 3127.
(9) Tran-Cong, Q.; Ohta, T.; Urakawa, O. *Phys. Rev. E* **1997**, *56*, R59.
(10) Harada, A.; Tran-Cong, Q. *Macromolecules* **1997**, *30*, 1643.
(11) Calvin, M.; Alter, H. W. *J. Chem. Phys.* **1951**, *19*, 765.
(12) (a) Cahn, J. W.; Hilliard, J. E. *J. Chem. Phys.* **1958**, *28*, 258. (b) Cahn, J. W. *Acta Metall.* **1961**, *9*, 795.
(13) Oono, Y.; Bahiana, M. *Phys. Rev. Lett.* **1988**, *61*, 1109. Bahiana, M.; Oono, Y. *Phys. Rev. A* **1990**, *41*, 6763.
(14) Liu, F.; Goldenfeld, N. *Phys. Rev. A* **1989**, *39*, 4805.
(15) Seul, M.; Andelman, D. *Science* **1995**, *267*, 476.
(16) Leibler, L. *Macromolecules* **1980**, *13*, 1602.
(17) Ohta, T.; Kawasaki, K. *Macromolecules* **1986**, *19*, 2621.
(18) For example, see: Saltiel, J.; D'Agostino, J.; Megarity, E. D.; Metts, L.; Neuberger, K. R.; Wrighton, M.; Zafiriou, O. C. In *Organic Chemistry*; Chapman, O. L., Ed.; Marcel Dekker: New York, 1973; Vol. 3.
(19) Irie, M.; Iga, R. *Makromol. Chem. Rapid Commun.* **1986**, *7*, 751.
(20) Urakawa, O.; Yano, O., Tran-Cong, Q.; Nakatani, A.; Han, C. C. *Macromolecules*, in press.
(21) Lifshitz, I. M.; Slyosov, V. V. *J. Phys. Chem. Solids* **1961**, *19*, 35.
(22) Wagner, C. *Z. Elektrochem.* **1961**, *65*, 581.
(23) Smets, G. *Adv. Polym. Sci.* **1983**, *50*, 17.
(24) (a) Sung, C. S. P.; Lamarre, L.; Tse, M. K. *Macromolecules* **1979**, *12*, 666. (b) Sung, C. S. P.; Lamarre, L.; Chung, K. H. *Macromolecules* **1981**, *14*, 1839.
(25) Williams, G.; Watts, D. C. *Trans. Faraday Soc.* **1970**, *66*, 80.
(26) Christensen, J. J.; Elder, K.; Fogedby, H. C. *Phys. Rev. E* **1996**, *54*, R2212.
(27) Verdasca, J.; Borckmans, P.; Dewel, G. *Phys. Rev. E* **1995**, *52*, R4616.
(28) Nakazawa, H.; Sekimoto, K. *J. Chem. Phys.* **1996**, *104*, 1675.

MA9803943